Viscoelasticity in two dimensions

G. P. Morriss and Denis J. Evans
Research School of Chemistry, Australian National University, Canberra, Australian Capital Territory 2601, Australia
(Received 4 April 1985)

We present the first nonequilibrium molecular-dynamics simulations of viscoelasticity in two-dimensional fluids. The shear viscosity is found to depend logarithmically upon the frequency; however, the divergence at low frequencies is shielded by a "turnover regime" where the shear viscosity becomes independent of frequency. The stress-stress autocorrelation function is shown to have a t^{-1} long-time tail, and the coefficient matches the coefficient of the logarithmic frequency dependence of the shear viscosity. The Goddard-Miller relation between the frequency and strain-rate dependence of the shear viscosity is shown to be incorrect. Superharmonic excitations are observed in both the shear stress and the pressure.

I. INTRODUCTION

Since the discovery of the "long-time tail" phenomena, hydrodynamics in two-dimensional systems has been a subject of considerable interest. The Green-Kubo relations predict that linear Navier-Stokes transport coefficients are given by infinite integrals of equilibrium time correlation functions.[1] These relations are generally thought to be exact. In two dimensions Alder and Wainwright[2] discovered that the Green-Kubo integrands for Navier-Stokes transport coefficients decay as t^{-1} at long times. Subsequently a wealth of theoretical evidence[3] has appeared which is in substantial agreement with computer-simulation calculations of Alder and Wainwright. The combination of theory and simulation supporting the divergence of the Green-Kubo formulas in two dimensions questions the validity of the Green-Kubo formulas. We have argued previously[4] that the derivation of Green-Kubo formulas for transport coefficients necessarily assumes the finiteness of the resulting expressions.

We have recently reported the results of computer simulations of the shear viscosity in two dimensions.[4] In contrast to earlier calculations, our recent results were obtained from nonequilibrium molecular-dynamics (NEMD) simulations of shear flow. These results are therefore independent of the validity, or otherwise, of the Green-Kubo formulas. In NEMD transport coefficients are calculated directly from their defining constitutive relations. These calculations suggest that planar Couette flow itself is unstable at small strain rates in two dimensions. The Green-Kubo relations which pertain to planar Couette flow might therefore be irrelevant in two dimensions. The NEMD calculation of the zero-frequency strain-rate-dependent shear viscosity shows that at small strain rates, the effective viscosity is finite and independent of strain rate (Newtonian). This contradicts the theoretical prediction of a logarithmic divergence.

A summary of the theoretical predictions for the behavior of the shear viscosity in two, three, and four dimensions are given below.

d	$\langle P_{xy}(t)P_{xy}\rangle$	$\mathrm{Re}[\tilde{\eta}(\omega)]$	$\eta(\gamma)$
2	t^{-1}	$-\log_{10}\omega$	$-\log_{10}\gamma$
3	$t^{-3/2}$	$\eta_0-A\omega^{1/2}$	$\eta_0-A\gamma^{1/2}$
4	t^{-2}	$\eta_0-A\omega$	$\eta_0-A\gamma$

The long-time behavior of the stress-stress autocorrelation function $\langle P_{xy}(t)P_{xy}\rangle$ has been observed in two dimensions[2] and three dimensions.[5] In both cases these Green-Kubo calculations were consistent with the mode-coupling functional forms given above. However, in both cases the observed amplitudes were orders of magnitude larger than theoretical predictions.

Nonequilibrium molecular dynamics has been used to study shear thinning $\eta(\gamma)$ in two, three, and four dimensions,[4–8] and viscoelasticity $\tilde{\eta}(\omega)$ in three dimensions.[6,7] An inverse Fourier-Laplace transform of $\tilde{\eta}(\omega)$ yields the time dependence of the memory function $\eta(t)$. If the Green-Kubo relations are correct this memory function is the equilibrium stress-stress autocorrelation function. In three dimensions agreement between the memory function and the autocorrelation function are excellent.[7] In this paper we perform a similar cross-check for two dimensional fluids.

The Goddard-Miller rheological equation of state[9,10] predicts that $\tilde{\eta}(\omega)=\eta(\gamma=\omega)$. In two dimensions the coefficient of the logarithmic dependence on strain rate should be the *same* as that for the logarithmic dependence on frequency.

II. MODEL AND ALGORITHM

The model system considered was the soft-disk fluid whose pair potential is

$$\phi(r)=\epsilon\left[\frac{\sigma}{r}\right]^{12}. \tag{1}$$

The state point studied was close to the freezing density, $\rho^*=\rho\sigma^2=0.8(\frac{4}{3})^{1/2}$. As the soft-disk equation of state is a function of one variable $X=\rho^*(T^*)^{-1/6}$ we chose

$T^*=kT/\epsilon=1$. This state point has been studied previously and the shear viscosity versus strain rate behavior, for reduced rates of unit or less, is known, as is its number dependence. Here we use a system of 896 soft disks with the potential cutoff at 1.5 σ. This allows the use of an efficient cell code algorithm.[11]

The correct algorithm for simulating planar Couette flow arbitrarily far from equilibrium is known as the sllod algorithm.[12] The results reported here use a combination of runs obtained using both the sllod algorithm and the dolls-tensor method.[13] Comparison of results derived using the two algorithms shows that the only statistically significant errors in the dolls-tensor calculations occur in the superharmonic excitations of the pressure tensor (see Sec. III). This is an interesting observation since at zero frequency it is only the normal stress differences which are incorrect with the dolls-tensor algorithm. For the dolls-tensor algorithm we have

$$\dot{\mathbf{q}}_i=\frac{1}{m}\mathbf{p}_i+\mathbf{n}_x\gamma(t)y_i \ , \tag{2}$$

$$\dot{\mathbf{p}}_i=\mathbf{F}_i-\mathbf{n}_y\gamma(t)p_{xi}-\alpha\mathbf{p}_i \ , \tag{3}$$

$$\alpha=\frac{\sum \mathbf{F}_i\cdot\mathbf{p}_i-\gamma(t)\sum p_{xi}p_{yi}}{\sum_i \mathbf{p}_i^2} \ , \tag{4}$$

where $\mathbf{n}_\lambda$ is a unit vector in the λ direction. The only change in isothermal sllod dynamics is to replace Eq. (3) by

$$\dot{\mathbf{p}}_i=\mathbf{F}_i-\mathbf{n}_x\gamma(t)p_{yi}-\alpha\mathbf{p}_i \ . \tag{5}$$

In both of these methods the momenta are interpreted as peculiar momenta and hence the temperature is defined to be

$$\frac{2NkT}{2}=\frac{1}{2m}\sum p_i^2 \ . \tag{6}$$

The isothermal constraint ensures that this temperature is kept constant, without explicit reference to its value. The necessary occasional velocity scaling which compensates for numerical drift ensures that the sum of the squares of the deviations from the linear profile are consistent with the temperature. This means that the deviation from linearity in the velocity profile at any instant in time is *only* due to thermal velocity. This stabilizes the linear velocity profile.

There are some extra boundary conditions associated with Eq. (2). When a particle's x coordinate moves outside the simulation cube its image appears according to the usually shearing boundary conditions. However, for both dolls-tensor and sllod dynamics it is necessary to recalculate $\dot{x}_i$ using Eq. (2), and with the Gear predictor-corrector algorithm all higher derivatives must also be recalculated.

For a system driven by a time-dependent force of frequency ω it is reasonable to assume that the response, as measured by $P_{xy}(t)$, is periodic with period $T=2\pi/\omega$. Therefore $P_{xy}(t)$ can be expanded in a Fourier series:

$$P_{xy}(t)=\tfrac{1}{2}a_0+\sum_{n=1}^{\infty}[a_n\cos(n\omega t)+b_n\sin(n\omega t)] \ , \tag{7}$$

where

$$a_n=\frac{2}{T}\int_0^T dt\, P_{xy}(t)\cos(n\omega t) \ , \tag{8}$$

$$b_n=\frac{2}{T}\int_0^T dt\, P_{xy}(t)\sin(n\omega t) \ . \tag{9}$$

Linear-response theory for an arbitrary phase variable B in a system undergoing shear gives

$$B(t)=\int_0^t ds\,\chi(t-s)\gamma(s) \ , \tag{10}$$

where the susceptibility χ is

$$\chi(t)=-\beta\langle B(t)P_{xy}(0)\rangle \ . \tag{11}$$

Clearly the right-hand side of Eq. (10) is a convolution, so in the frequency domain

$$\tilde{B}(\omega)=\tilde{\chi}(\omega)\tilde{\gamma}(\omega) \tag{12}$$

and a system driven at a frequency ω will respond at that frequency *only*. In practice however, the nonlinear response of the system can be expected to contain contributions from higher harmonics of the driving frequency. When P_{xy} is chosen to be the response function, the real part of the complex susceptibility $\tilde{\chi}(\omega)$ is the frequency-dependent shear viscosity. The nonequilibrium molecular-dynamics method then consists of driving the system at a fixed frequency ω, and monitoring the response of P_{xy} at the same frequency. The frequency-dependent shear viscosity is calculated from Eq. (12).

In an isothermal nonequilibrium molecular-dynamics simulation there is a second route to the frequency-dependent shear viscosity. We consider the energy dissipation in the system $\dot{H}_0$ where

$$H_0=\frac{1}{2m}\sum_i \mathbf{p}_i^2+\Phi \ . \tag{13}$$

From either the dolls-tensor equations of motion or inverse dynamics it is straightforward to show that

$$\dot{H}_0(t)=-P_{xy}(t)V\gamma(t)-2NkT\alpha(t) \ . \tag{14}$$

If the system is in a steady state then the dissipation over a period of the driving frequency is zero [or equivalently $H_0(t)$ has period $2\pi/\omega$] so

$$\mathrm{Re}[\tilde{\eta}(\omega)]=4\rho kT\langle\alpha\rangle/\gamma^2 \ . \tag{15}$$

This is the second independent route to the viscosity.

III. RESULTS

Nonequilibrium molecular-dynamics simulations were performed at two values of the strain rate ($\gamma=0.1$ and 1.0) for a range of values of the frequency. In Figs. 1(a) and 2(a) we see that the real part of the susceptibility $\tilde{\chi}(\omega)$ is linear in the logarithm of the frequency. At higher frequencies it decays rapidly to zero, while at low frequencies there is a "turnover" region in which $\tilde{\eta}(\omega)$ is essentially independent of frequency. This behavior at low frequency is consistent with the turnover regime of $\eta(\gamma)$ at low strain rates.[4] Evidently $\tilde{\eta}(\gamma,\omega)$ is independent of *both* γ and ω when frequency and strain rate are "small." Also

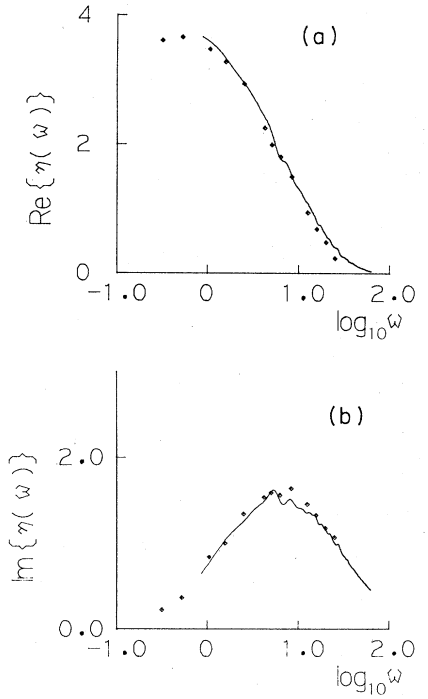

FIG. 1. Real (a) and imaginary (b) parts of the shear viscosity at the driving frequency ω, and a strain rate of $\gamma=0.1$ [$-a_1/\gamma$, see Eq. (7)]. Points are the NEMD results while the line is from the Fourier-Laplace transform of the equilibrium stress-stress autocorrelation function.

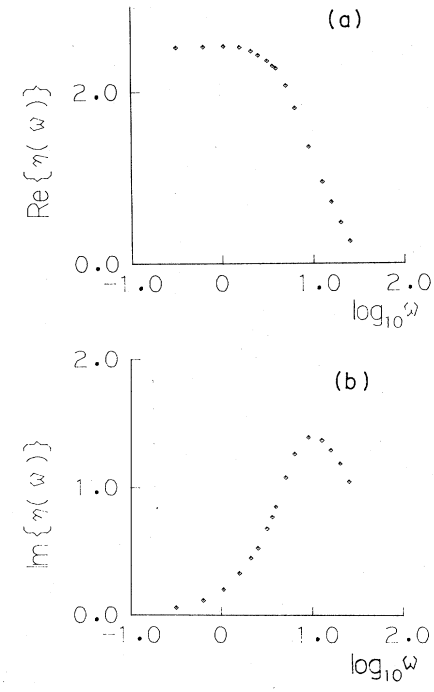

FIG. 2. Real (a) and imaginary (b) parts of the shear viscosity at the driving frequency ω, and a strain rate of $\gamma=1$ by NEMD.

shown in Figs. 1(a) and 1(b) are the real and imaginary parts of the Fourier-Laplace transform of the equilibrium stress-stress autocorrelation function. As this represents the limit as $\gamma\to 0$ of $\tilde{\eta}(\gamma,\omega)$, we see that there is no change in the real or imaginary part of the susceptibility between $\gamma=0$ and 0.1. In fact the only change we observe in going from $\gamma=0.1$ to 1.0 is that the low-frequency limit or "turnover value" falls. It is not possible to conclude much about the existence of the turnover region from the numerical Fourier-Laplace transform of the stress-stress autocorrelation function. The Green-Kubo calculations are simply too difficult to derive spectral data at the turnover frequency. The numerical transform has been plotted only for the range of values of frequency for which the data are reliable. Wainwright, Alder, and Gass[2] have shown, however, for the much simpler hard-disk system, that the Laplace transform of the stress autocorrelation function is logarithmic to frequencies which extend into the turnover regime shown in Fig. 1. There is no Green-Kubo simulation data suggesting the existence of the turnover regime. Its existence in the results of NEMD simulations suggests that the Green-Kubo formulas are invalid in this regime. For frequencies above the turnover frequency the agreement between Green-Kubo and NEMD is excellent.

The imaginary part of the Fourier-Laplace transform shown in Fig. 1(b) is also in excellent agreement with the NEMD results. The only change in going from $\gamma=0.1$ to 1.0 is that the maximum of this function shifts to higher frequency.

The Green-Kubo expression for the frequency-dependent shear viscosity is

$$\tilde{\eta}(\omega)=\frac{V}{kT}\int_0^\infty dt\langle P_{xy}(t)P_{xy}(0)\rangle_0 e^{-i\omega t}\,. \tag{16}$$

This expression relates the spectrum of fluctuations in an equilibrium simulation to $\tilde{\eta}(\omega)$; however, the stress-stress autocorrelation function is believed to have a power-law decay at long time ($t^{-d/2}$ where d is the dimensionality of the system). In two dimensions this decay implies that if

$$\frac{V}{kT}\langle P_{xy}(t)P_{xy}(0)\rangle\sim At^{-1}\ \text{ as } t\to\infty \tag{17}$$

then

$$\tilde{\eta}(\omega)\sim -A\ln\omega\ \text{ as } \omega\to 0\,, \tag{18}$$

where the coefficients A in Eqs. (17) and (18) are the *same*.

The Goddard-Miller rheological equation of state[9] predicts that in both two and three dimensions the coefficient of the leading functional dependence on strain rate should be the same as the coefficient of the leading functional dependence on frequency. That is,

$$\eta(\gamma)\sim -A\ln\gamma\ \text{ as } \gamma\to 0\,. \tag{19}$$

It has already been shown that this is not obeyed in three dimensions,[9,7] and here we show that it also fails in two dimensions.

In Fig. 3 we show the equilibrium stress-stress autocorrelation function plotted against $1/t$. Clearly it is

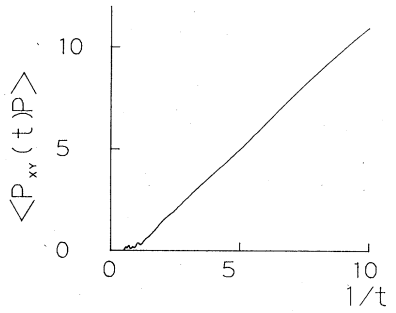

FIG. 3. Equilibrium stress-stress autocorrelation function plotted against the inverse time. Linear region near the origin is the t^{-1} long-time tail.

linear in $1/t$ for reduced times longer than $t=0.125$. The coefficient is estimated to be 1.24 ± 0.06. Formally we know that this long-time behavior implies that the frequency dependence of $\tilde{\eta}(\omega)$ at $\gamma=0$ is logarithmic. However, it is reasonable to expect that at nonzero strain rates the logarithmic behavior will remain. This is indeed the case with the coefficient of $-\ln\omega$ being 1.23 ± 0.10 at $\gamma=0.1$, and 1.22 ± 0.10 at $\gamma=1.0$. Clearly the logarithmic behavior at fixed nonzero strain rates is completely consistent with the $1/t$ long-time correlation function; however, we note that $-\ln\omega$ is not the limiting low-frequency behavior and the logarithmic divergence is shielded by a turnover regime as in the zero-frequency low-strain-rate regime.

Previously we have studied the viscosity as a function of strain rate[4] and an analysis of that data gives

$$\eta(\gamma)\sim-0.55\ln\gamma\ . \tag{20}$$

The coefficient in the strain rate domain is less than half the value of the coefficient in the frequency domain. This is the converse of the three-dimensional result.[9]

In the zero-frequency shear viscosity NEMD simulations the strain rate couples, not only to quantities with the same tensorial character, but to other properties, for example the pressure (shear dilatancy). (At fixed strain rates the frequency also couples to the pressure.) The shear dilatancy Δp is defined to be the difference between the pressure at fixed strain rate and frequency, and its equilibrium value $\langle p\rangle_0$. At a frequency ω we can expand the pressure as a Fourier series, so that $\Delta\tilde{p}$ is given by

$$\Delta\tilde{p}(\gamma,\omega)=\lim_{X\to\infty}\frac{1}{X}\int_0^X dt\left[\tfrac{1}{2}a_0+\sum_{n=1}^{\infty}[a_n\cos(n\omega t)+b_n\sin(n\omega t)]\right]-\langle p\rangle_0\ . \tag{21}$$

The limit $\omega\to0$, however, does not commute with the limit $X\to\infty$ as

$$\lim_{\omega\to0}\lim_{X\to\infty}\Delta\tilde{p}(\gamma,\omega;X)=\tfrac{1}{2}\langle a_0\rangle-\langle p\rangle_0$$

and

$$\lim_{X\to\infty}\lim_{\omega\to0}\Delta\tilde{p}(\gamma,\omega;X)=\tfrac{1}{2}\langle a_0\rangle+\sum_{n=1}^{\infty}\langle a_n\rangle-\langle p\rangle_0\ .$$

To resolve this difficulty we consider the implication of these limits upon the equations of motion, Eqs. (2)—(5). Taking the limit $X\to\infty$ first implies that the time average of the driving force $\gamma_0\cos(\omega t)$ is zero and in a sense the equations of motion are "on average" Newtonian. However, if the limit $\omega\to0$ is taken first at fixed finite X, then the equations of motion reduce to the frequency-independent equations *everywhere* in the time interval 0 to X. In order to ensure consistency as $\omega\to0$, we take

$$\Delta\tilde{p}(\gamma,\omega)=\tfrac{1}{2}\langle a_0\rangle+\sum_{n=1}^{\infty}\langle a_n\rangle-\langle p\rangle_0 \tag{22}$$

as the definition of the shear dilatancy at *all frequencies.* In Fig. 4 we plot the shear dilatancy as a function of frequency at a shear rate of 1.0. The point on the y axis is the zero-frequency result at the same strain rate. The shear dilatancy appears to rise to a weak maximum at a frequency equal to the strain rate. This may be the result of the so-called "double resonance" effect.

Linear-response theory, as discussed earlier, predicts that a system driven at a frequency ω will respond at that frequency only. Interestingly, we find in this work that at a shear rate of 1.0 the shear stress responds strongly at a frequency of 3ω and the pressure at a frequency of 2ω. Indeed it appears that properties which are even in the sign of the strain rate (for example, the pressure) respond at even multiples of the driving frequency, while properties which are odd in the sign of the strain rate respond at odd multiples of the driving frequency. Although previous attempts have been made, this is the first time these superharmonic stress excitations have been observed in computer simulations. In Fig. 5 we show the real and imaginary parts of the shear stress at 3ω, that is, a_3 and b_3 in the Fourier expansion of $P_{xy}(t)$. Both show behavior which is similar to that of the response at ω, except that both have a negative region. The response at 2ω is essentially zero as $|a_2|<0.0136$ and $|b_2|<0.018$ which is statistically indistinguishable from zero.

In Fig. 6 we present the response of the second harmonic of the pressure at a shear rate of 1.0. Once again the frequency dependence is very similar to the frequency dependence of $P_{xy}(t)$ at ω; with a turnover regime followed by a logarithmic decay in the real part, and a max-

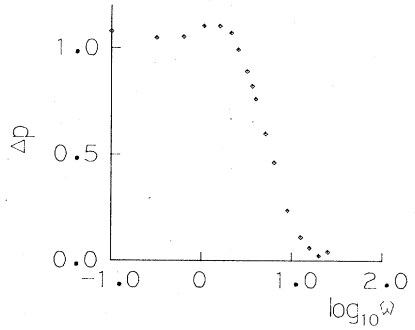

FIG. 4. Shear dilatancy at a strain rate of $\gamma=1$ as a function of frequency using Eq. (2) by NEMD.

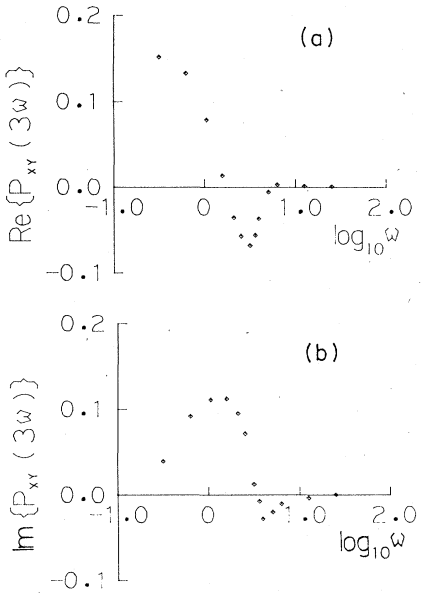

FIG. 5. Real (a) and imaginary (b) parts of the third harmonic of the shear stress at a strain rate of $\gamma=1$ by NEMD.

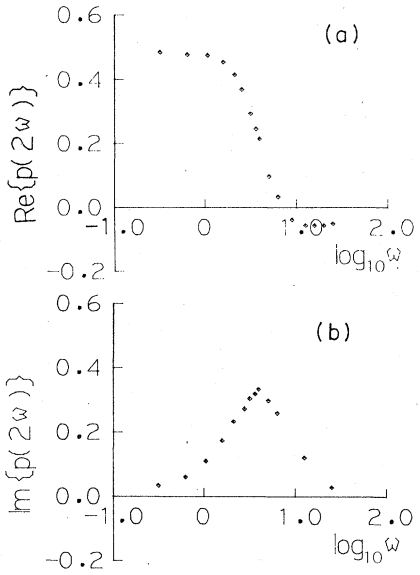

FIG. 6. Real (a) and imaginary (b) parts of the second harmonic of the pressure at a strain rate of $\gamma=1$ by NEMD.

imum at about $\omega=4$ in the imaginary part. The response at ω is again indistinguishable from zero with $|a_1|<0.010$ and $|b_1|<0.015$. It is interesting to note that the superharmonic responses do not appear to vanish as the frequency tends to zero.

Superharmonic response is a strictly nonlinear effect and hence is strongly related to the strain rate. At the lower strain rate of 0.1 similar response is present, however, the signal to noise ratio is much smaller. sllod dynamics gives values of the imaginary part of the shear stress at 3ω (that is, b_3) which are larger than those obtained using the dolls-tensor method. For example, at $\omega=1.57$ and 1.05, dolls tensor gives b_3 to be ~ 0.11 whereas sllod dynamics gives b_3 to be ~ 0.13. For all the other superharmonics the two methods agree to within statistical uncertainty.

IV. CONCLUSIONS

Our NEMD results for $\tilde{\eta}(\omega)$ seem to be at odds with earlier calculations via the Green-Kubo formulas.[2] The earlier calculations apparently show no evidence for the turnover observed in the present work. Unfortunately the limited computational facilities at the Australian National University do not allow us to perform accurate low-frequency Green-Kubo calculations to check Wainwright and Alder's hard-sphere data. We hope that others may be stimulated to perform these checks.

Assuming the Wainwright-Alder Green-Kubo data are accurate and transferable to our soft-disk system, it is possible that the apparent contradiction with our NEMD data might be resolved. The Green-Kubo formulas are either inaccurate or inapplicable to two-dimensional Couette flow at sufficiently small strain rates and frequencies. After all, their correctness rests on the existence of *finite* transport coefficients which they subsequently predict to be *infinite*. The actual low-frequency behavior observed in NEMD is not logarithmic and it appears that in two dimensions the shear viscosity becomes independent of both the shear rate γ and frequency ω, for $\gamma<0.1$ and $\omega<1$, for the state considered here. The Goddard-Miller prediction that the coefficient of the logarithmic frequency dependence should be equal to the coefficient of the logarithmic shear-rate dependence is shown to be false, as the coefficients differ by more than a factor of 2.

For the first time in a computer simulation we have observed superharmonic excitations in both the shear stress, at 3ω, and the pressure, at 2ω. This is clearly a nonlinear effect as linear-response theory connects the driving force and the response at the same frequency only. As yet no theory exists for these superharmonic excitations, but as this is a purely nonlinear effect, this may be a useful test of nonlinear theories as it is not necessary to use extreme values of the driving force to observe it (thus avoiding the possibility of saturation effects in the response).

[1]P. Resibois and M. de Leener, *Classic Kinetic Theory of Fluids* (Wiley, New York, 1977), p. 363.

[2]B. J. Alder and T. E. Wainwright, Phys. Rev. A **1**, 18 (1970); Phys. Rev. Lett. **18**, 988 (1967); B. J. Alder, D. M. Gass, and T. E. Wainwright, J. Chem. Phys. **53**, 381 (1970); T. E. Wainwright, B. J. Alder, and D. M. Gass, Phys. Rev. A **4**, 233 (1970).

[3]K. Kawasaki and J. D. Gunton, Phys. Rev. A **8**, 2048 (1973); T. Yamada and K. Kawasaki, Prog. Theor. Phys. **53**, 111 (1975); M. H. Ernst, B. Cichocki, J. R. Dorfman, J. Sharma, and H. van Beijeren, J. Stat. Phys. **18**, 237 (1978).

[4]D. J. Evans and G. P. Morriss, Phys. Rev. Lett. **51**, 1776 (1983).

[5]W. Wood and J. Erpenbeck, J. Stat. Phys. **24**, 455 (1981).

[6]D. J. Evans, J. Stat. Phys. **22**, 81 (1980).

[7]D. J. Evans, Phys. Rev. A **22**, 290 (1980).

[8]D. J. Evans, Phys. Lett. **101A**, 100 (1984).

[9]R. Zwanzig, Proc. Natl. Acad. Sci. U.S.A. **78**, 3296 (1981).

[10]R. B. Bird, R. C. Armstrong, and Q. Hassager, Fluid Mechanics (Wiley, New York, 1977), Vol. 1.
[11]D. J. Evans and G. P. Morriss, Comput. Phys. Rep. **1**, 297 (1984).
[12]A. J. C. Ladd, Mol. Phys. **53**, 459 (1984); D. J. Evans and G. P. Morriss, Phys. Rev. A **30**, 1528 (1984).
[13]W. G. Hoover, D. J. Evans, R. B. Hickman, A. J. C. Ladd, W. T. Ashurst, and B. Moran, Phys. Rev. **22**, 1690 (1980).